Mathematics and Systems Science 2025, 3(2), 3148.
https://doi.org/10.54517/mss3148

Article

Some applications of partial differential equations in medical image processing

Bassam Al-Hamzah[1,*], **Fahmi Al-Hamzah**[2]

[1] Department of Mathematics, University of Saba Region, Marib 55311, Yemen
[2] Hamad Medical Corporation, Doha 93151, Qatar
* **Corresponding author:** Bassam Al-Hamzah, bassamalhamzah@yahoo.com

CITATION

Al-Hamzah B, Al-Hamzah F. Some applications of partial differential equations in medical image processing. Mathematics and Systems Science. 2025; 3(2): 3148. https://doi.org/10.54517/mss3148

ARTICLE INFO

Received: 9 December 2024
Accepted: 6 February 2025
Available online: 8 April 2025

Abstract: The second-order nonlinear diffusion parabolic partial differential equations models have been widely applied in image restoration. However, the numerical results in the literature treat only the case without source term. In this paper, we have developed a general calculation code which is based in a consistent explicit approximation finite difference method scheme. Furthermore, the paper provides satisfying answers with a nonlinear source term relying on the image solution and its gradient. Numerical experiments are presented to show the robustness of the cases with source term to obtain better results in image denoising restoration using measures as Peak Signal-to-Noise Ratio (PSNR) and SNR of filtering and noisy image.

Keywords: nonlinear parabolic; reaction-diffusion; medical image processing

1. Introduction

The Perona-Malik equation, introduced in 1987 [1], is seen as among the earliest efforts to derive a model incorporating local information within a PDE framework. It has sparked significant interest within the image processing community [2–9]. Perona and Malik developed a nonlinear diffusion model, termed 'anisotropic' to address issues such as edge blurring localization problems that arise in linear diffusion models. They implemented a diffusion process where the diffusivity is guided by derivatives of the evolving image. The formulation that has garnered considerable interest is the mathematically rigorous one by Catté et al. [10], which we will elaborate on in the second section.

Althoug nonlinear second-order PDEs successfully address the limitations of traditional 2D filters by preventing image blurring, preserving the edges effectively, and exhibiting good localization properties, they frequently suffer from another undesirable effect: the so-called staircase, or blocky, effect. In recent years, numerous second-order nonlinear diffusion-based restoration techniques have been proposed to mitigate this effect. Notable examples include various enhanced versions of the Perona-Malik algorithm and TV denoising, such as those discussed in [2,6,9].

In this paper, we summed up the existing nonlinear diffusion models and theoretical results on existence and uniqueness in the literature [2, 8, 11–14]. The Section 3, a consistent explicit numerical approximation scheme based on the finite difference method has been developed for the proposed PDE models. We use an explicit scheme with Dirichlet, Neumann boundary conditions. In Section 4, the nonlinear second-order diffusion-based filtering technique proposed here has been tested on some medical images affected by Gaussian noise, salt and pepper and

Speckle noises, satisfactory restoration results being achieved by using measures as Peak Signal-to-Noise Ratio (PSNR) of filtering and noisy image.

2. Nonlinear diffusion models in image processing

In 2009, the study of Morfu [15] was focused on the contrast enhancement and noise filtering. He considers the Fisher equation, which generally allows simulating the transport mechanisms in living cells, but also enhances the contrast and segmenting images.

After that in 2014, the work of Noureddine Alaa et al. [11] are to modify the model of Morfu . The proposed model is as follows:

$$\begin{cases} \frac{\partial u}{\partial t} - \mathrm{div}[g(|\nabla u_\sigma|)\nabla u] = f(t,x,u) \text{ in } Q_T \\ u(0,x) = u_0(x) \geq 0 \text{ in } \Omega \\ \frac{\partial u}{\partial \nu} = 0 \text{ on } \Sigma_T \end{cases} \tag{1}$$

where $\Omega\ =]0,1[\times]0,1[$, $Q_T\ =]0,T[\times\Omega$ and $\Sigma_T\ =]0,T[\times\partial\Omega$, where $(T > 0)$, $G_\sigma(x) = \frac{1}{\sqrt{2\pi\sigma}}e^{-(\frac{|x|^2}{4\sigma})}, x \in \mathbb{R}^2, \sigma > 0$ and $\nabla u_\sigma = \nabla(u * G_\sigma) = u * \nabla G_\sigma$.

The general case $f = (t,x,u,\nabla u)$ was treated by Al-hamzah and Yebari [13] under the following assumptions:

(H_g) $g : [0,+\infty[\to [0,+\infty[$ is a smooth non-increasing function, where $g(0) > 0$ and $\lim_{s\to+\infty} g(s) = 0$.
$(H_f)_1$ $f : Q_T \times \mathbb{R} \times \mathbb{R}^N \to \mathbb{R}$ is measurable and $f(t,x,...) : \mathbb{R}\times\mathbb{R}^N \to \mathbb{R}$ are locally Lipshitz continuous: ($\exists r > 0$, for almost $(t,x) \in Q_T/\ |f(t,x,u,p) - f(t,x,\hat{u},\hat{p})| \leq M(r)[|u-\hat{u}| + \|p-\hat{p}\|]$) for all $0 \leq |u|, |\hat{u}|, \|p\|, \|\hat{p}\| \leq r$. $(H_f)_2$ for almost $(t,x) \in Q_T$, $f(t,x,0,0) \geq 0$.
$(H_f)_3$ $\forall(u,p) \in \mathbb{R}\times\mathbb{R}^N$ and for almost $(t,x) \in Q_T$, $uf(t,x,u,p) \leq 0$.
$(H_f)_4$ $|f(t,x,u,\nabla u)| \leq C(|u|)[F(t,x) + |\nabla u|^2]$ where $C : [0,+\infty[\to [0,+\infty[$ is non-decreasing, $F \in L^1(Q_T)$ and $|\nabla u|^2 = (\frac{\partial u}{\partial x_1})^2 + (\frac{\partial u}{\partial x_2})^2$.
Remark 1. *A typical examples where the result of this paper can be applied are*
(i) Three of the diffusivity Perona and Malik [1] *are*

$$g(s) = \frac{1}{1+s^2} + \alpha,\ g(s) = \frac{1}{\sqrt{1+s^2}} + \alpha,\ or\ g(s) = exp(-(1+\frac{s}{\lambda})) + \alpha$$

where λ is a threshold (contrast) parameter that separates forward and backward diffusion, α is a threshold (contrast) parameter in the work of (*Aboulaich* et al. [1]).
(ii) $f(t,x,u,\nabla u) = -\beta u(u-a)^{2\tau}(1-u)^{2\gamma} + a_{11}u|\nabla u|^\tau, 1 \leq \tau < 2,$ *where* $\beta,\gamma > 0$, $\tau,\gamma \neq \frac{1}{2}$ *and* $0 < a < 1, a_{11} \leq 0$.

3. Discretisation

In this section, the proposed nonlinear diffusion model is discretized by using the finit-difference method, a consistent explicit numerical approximation scheme is developed for the proposed PDE models.

The case $K(u) = g(|\nabla u|)$. For the temporal discretization of the time derivative we have:

$$\frac{\partial u}{\partial t}(i,j) = \frac{u^{n+1}(i,j) - u^n(i,j)}{dt}$$

dt time steps size, for the discrete divergence approximation:

$$\text{div}(K(u^n)\nabla u^n) = \frac{\partial}{\partial x}(K(u^n)\frac{\partial u^n}{\partial x}) + \frac{\partial}{\partial y}(K(u^n)\frac{\partial u^n}{\partial y})$$

suppose $\frac{\partial}{\partial x}(K(u^n)\frac{\partial u^n}{\partial x}) = D_{xx}u^n$

$$K_{xp} = k_x(u^n)_{i+\frac{1}{2}} = \frac{K(u^n)(i+1,j) + K(u^n)(i,j)}{2}$$

$$K_{xm} = k_x(u^n)_{i-\frac{1}{2}} = \frac{K(u^n)(i,j) + K(u^n)(i-1,j)}{2}$$

and

$$[\frac{\partial}{\partial x}u^n]^+(i,j) = D_x u_p^n = \frac{u^n(i+1,j) - u^n(i,j)}{dx}$$

$$[\frac{\partial}{\partial x}u^n]^-(i,j) = D_x u_m^n = \frac{u^n(i,j) - u^n(i-1,j)}{dx}$$

that leads to

$$\frac{\partial}{\partial x}(K(u^n)\frac{\partial u^n}{\partial x})(i,j) = D_{xx}u^n(i,j) = \frac{k_x(u^n)_{i+\frac{1}{2}}[\frac{\partial}{\partial x}u^n]^+(i,j) - k_x(u^n)_{i-\frac{1}{2}}[\frac{\partial}{\partial x}u^n]^-(i,j)}{dx}$$

suppose $\frac{\partial}{\partial y}(K(u^n)\frac{\partial u^n}{\partial y}) = D_{yy}u^n$

$$K_{yp} = k_y(u^n)_{i+\frac{1}{2}} = \frac{K(u^n)(i,j+1) + K(u^n)(i,j)}{2}$$

$$K_{ym} = k_y(u^n)_{i-\frac{1}{2}} = \frac{K(u^n)(i,j) + K(u^n)(i,j-1)}{2}$$

and

$$[\frac{\partial}{\partial y}u^n]^+(i,j) = D_y u_p^n = \frac{u^n(i,j+1) - u^n(i,j)}{dy}$$

$$[\frac{\partial}{\partial x}u^n]^-(i,j) = D_y u_m^n = \frac{u^n(i,j) - u^n(i,j-1)}{dy}$$

that leads to

$$\frac{\partial}{\partial y}(K(u^n)\frac{\partial u^n}{\partial y})(i,j) = D_{yy}u^n(i,j) = \frac{k_y(u^n)_{i+\frac{1}{2}}[\frac{\partial}{\partial y}u^n]^+(i,j) - k_y(u^n)_{i-\frac{1}{2}}[\frac{\partial}{\partial y}u^n]^-(i,j)}{dy}$$

Finally, we obtain the explicit scheme

$$u^{n+1}(i,j) = u^n(i,j) + dt(D_{xx}u^n(i,j) + D_{yy}u^n(i,j)) + dt(f^n(i,j))$$

where

$f^n(i,j) = f(x_i, y_j, t_n), u^n(i,j) = u(x_i, y_j, t_n), x_i = (i-1)dx, y_j = (j-1)dy,$ $t_n = (n-1)dt,\ n = 1, ..., nt$ where $nt-1 = \frac{t_{end}}{dt}$, $i = 2$ to $nx-1$, and $j = 2$ to $ny-1$.

Boundary conditions, Neumann conditions

$u(i,1) = u(i,2)$, where $2 \leq i \leq nx-1$ we have

$$u^{n+1}(i,1) = u^n(i,2) + dt(D_{xx}u^n(i,2) + D_{yy}u^n(i,2)) + dt(f^n(i,2))$$

$u(i,ny) = u(i,ny-1)$, $2 \leq i \leq nx-1$ we have

$$u^{n+1}(i,ny) = u^n(i,ny-1) + dt(D_{xx}u^n(i,ny-1) + D_{yy}u^n(i,ny-1)) + dt(f^n(i,ny-1))$$

$u(1,j) = u(2,j)$, where $2 \leq j \leq ny-1$ we have

$$u^{n+1}(1,j) = u^n(2,j) + dt(D_{xx}u^n(2,j) + D_{yy}u^n(2,j)) + dt(f^n(2,j))$$

$u(nx,j) = u(nx-1,j)$, $2 \leq j \leq ny-1$ we have

$$u^{n+1}(nx,j) = u^n(nx-1,j) + dt(D_{xx}u^n(nx-1,j) + D_{yy}u^n(nx-1,j)) + dt(f^n(nx-1,j))$$

4. Experiments for medical images

The nonlinear second-order diffusion-based filtering technique proposed here has been tested on some medical images affected by Gaussian noise, salt and pepper and Speckle noises, satisfactory restoration results being achieved. We obtain the best results for the nonlinear models on images filtering and noises for $\alpha = 0$, on all type of filters presenting in the literature [2,14,16] and the case $f = -u(1-u)^2 - u|\nabla u|$. With

$$g(s) = \frac{1}{1+s^2} + \alpha,\ g(s) = \frac{1}{\sqrt{1+s^2}} + \alpha,\ \text{or } g(s) = exp(-(1+\frac{s}{\lambda})) + \alpha$$

where λ is a threshold (contrast) parameter that separates forward and backward diffusion.

We remark that the model proposed by Aboulaich et al. [2] gives a better solution for a small values of α and they had taken $h = dx = dy = 1$. While in this work we get better results for $\alpha = 0$ **Figures 1** and **2**. As shown in **Figures 3** and **4**, we obtain bad image restoration when setting large α. The performance of this PDE filtering approach has been assessed by using measures as Peak Signal-to-Noise Ratio (PSNR). the values provided by our technique and other filtering approaches are displayed in **Tables 1–4**. One can see the convolution with the Gaussian filter G_σ, represents the best enhancement result, with $g(s) = exp(-(1+\frac{s}{\lambda}))$, where $\lambda = 0.01$.

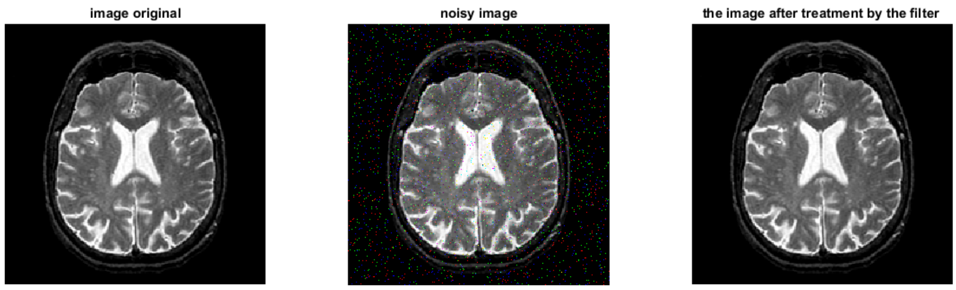

Figure 1. Influence of the parameter $\alpha = 0$ on the restored image after noise-type (salt and pepper).

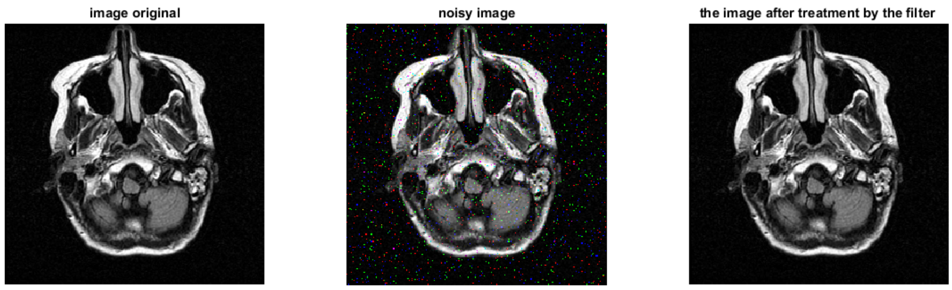

Figure 2. Influence of the parameter $\alpha = 0$ on the restored image after noise-type (salt and pepper).

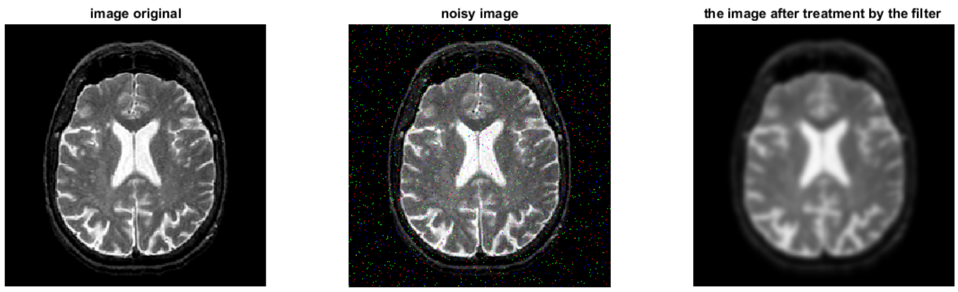

Figure 3. Influence of the parameter $\alpha = 10$ on the restored image.

Figure 4. Influence of the parameter $\alpha = 10$ on the restored image.

PSNR values achieved by the nonlinear restoration method are displayed In the following tables.

Some restoration results provided by these techniques are displayed in **Figure 1**. The original $[443 \times 443]$. The results produced by the $[3 \times 3]$, 2D filters.

Table 1. Evaluation of the noise suppression by the nonlinear restoration method.

		$g(s) = \frac{1}{1+s^2}$	$g(s) = \frac{1}{\sqrt{1+s^2}}$	$g(s) = e^{-(1+\frac{s}{\lambda})}$	σ
$f = 0$	PSNR	20.8626	20.7568	20.7528	0.0090
	SNR	11.0666	10.9608	10.9568	
$f = 1 - u^2$	PSNR	20.7948	20.7247	20.7070	0.0090
	SNR	10.9988	10.9287	10.9110	
$f = -u(1-u)^2 - u\lvert\nabla u\rvert$	PSNR	20.8305	20.7638	20.7574	0.0090
	SNR	11.0345	10.9679	10.9614	

Some restoration results provided by these techniques are displayed in **Figure 2**.

The original $[256 \times 256]$. The results produced by the $[3 \times 3]$, 2D filters.

Table 2. Evaluation of the noise suppression by the nonlinear restoration method.

		$g(s)=\frac{1}{1+s^2}$	$g(s)=\frac{1}{\sqrt{1+s^2}}$	$g(s)=e^{-(1+\frac{s}{\lambda})}$	σ
$f=0$	PSNR	20.8880	20.6875	20.6362	0.9000
	SNR	10.6348	10.4343	10.3831	
$f=1-u^2$	PSNR	20.7390	20.8943	20.6852	0.0090
	SNR	10.4859	10.6411	10.4321	
$f=-u(1-u)^2-u\|\nabla u\|$	PSNR	20.8859	20.7015	20.6495	0.0090
	SNR	10.6328	10.4483	10.3963	

Some restoration results provided by these techniques are displayed in **Figure 3**. The original $[607 \times 607]$. The results produced by the $[3 \times 3]$, 2D filters.

Table 3. Evaluation of the noise suppression by the nonlinear restoration method.

		$g(s)=\frac{1}{1+s^2}$	$g(s)=\frac{1}{\sqrt{1+s^2}}$	$g(s)=e^{-(1+\frac{s}{\lambda})}$	σ
$f=0$	PSNR	21.6877	21.6718	21.6569	0.9950
	SNR	15.0082	14.9924	14.9774	
$f=1-u^2$	PSNR	21.7085	21.6550	21.6348	0.9500
	SNR	15.0290	14.9756	14.9553	
$f=-u(1-u)^2-u\|\nabla u\|$	PSNR	21.6978	21.7412	21.6544	0.0100
	SNR	15.0184	15.0618	14.9749	

Some restoration results provided by these techniques are displayed in **Figure 4**. The original $[512 \times 512]$. The results produced by the $[3 \times 3]$, 2D filters.

Table 4. Evaluation of the noise suppression by the nonlinear restoration method.

		$g(s)=\frac{1}{1+s^2}$	$g(s)=\frac{1}{\sqrt{1+s^2}}$	$g(s)=e^{-(1+\frac{s}{\lambda})}$	σ
$f=0$	PSNR	20.7650	20.7397	20.7007	0.0002
	SNR	12.5775	12.5523	12.5132	
$f=1-u^2$	PSNR	20.7790	20.6878	20.6865	0.0002
	SNR	12.5916	12.5004	12.4991	
$f=-u(1-u)^2-u\|\nabla u\|$	PSNR	20.7794	20.7323	20.7236	0.0010
	SNR	12.5920	12.5449	12.5361	

5. Conclusion

This paper develops a general calculation code for testing all type of filters presenting in the literature [2,14]. To the best of our knowledge, the numerical results in the literature treat only the case without source term. This work provides satisfying answers with a nonlinear source term relying on the image solution and its gradient.

The method introduced in this paper has been validated by comparing the exact solution with the numerical solution. Furthermore, a consistent explicit numerical approximation scheme based on the finite difference method has been developed for the proposed PDE models. The result showed that the cases with source term are the most accurate models appears using measures as Peak Signal to-Noise Ratio (PSNR) of filtering and noisy image, as shown in **Tables 1–4**, and **Figures 1–4**.

Author contributions: Conceptualization, BAH and FAH; methodology, BAH and FAH; software, BAH and FAH; validation, BAH and FAH; formal analysis, BAH and FAH; investigation, BAH and FAH; resources, BAH and FAH; data curation, BAH and FAH; writing—original draft preparation, BAH and FAH; writing—review and editing, BAH and FAH; visualization, BAH and FAH; supervision, BAH and FAH; project administration, BAH and FAH; funding acquisition, BAH and FAH. All authors contributed equally to the writing of this paper. All authors have read and agreed to the published version of the manuscript.

Institutional review board statement: Not applicable.

Informed consent statement: Not applicable.

Conflict of interest: The authors declares no conflict of interest.

References

1. Perona P, Malik J. Scale-space and edge detection using anisotropic diffusion. IEEE Transactions on Pattern Analysis and Machine Intelligence. 1990; 12(7): 629–639.
2. Aboulaich R, Boujena S, Guarmah EE. A Nonlinear Parabolic Model in Processing of Medical Image. Math. Model. Nat. Phenom. 2008; 3(6): 131–145.
3. Alvarez L, Guichard F, Lions PL, Morel JM. Axioms and fundamental equations of image processing. Archive for Rational Mechanics and Analysis. 1993; 123: 199–257.
4. Alvarez L, Mazorra L. Signal and image restoration using shock filters and anisotropic diffusion. SIAM Journal on Numerical Analysis. 1994; 31(2): 590–605.
5. Amann H, Crandall MG. On some existence theorems for semi linear equations. Indiana Univ. Math. J. 1978; 27(5): 779–790.
6. Benila P, Brezis H. Weak solutions of evolution equations in Hilbert spaces (French). Ann. Inst. Fourier. 1972; 22: 311–329.
7. Ladyzheuskaya OA, Solonnikov VA, Ural'tseva NN. Linear and Quasi Linear Equations of Parabolic Type. Amer Mathematical Society Publishing; 1995.
8. Peng Y, Pi L, Shen C. A semi-automatic method for burn scar delineation using a modified chan-vese model. Computer and Geosciences. 2009; 35(2): 183–190.
9. Zhang K. Existence of infinitely many solutions for the one-dimensional Perona-Malik model. Calculus of Variations and Partial Differential Equations. 2006; 26: 171–199.
10. Catté F, Lions PL, Morel JM, Coll T. Image Selective Smoothing and Edge Detection by Nonlinear Diffusion. SIAM Journal on Numerical Analysis. 1992; 29(1): 182–193.
11. Alaa N, Aitoussous M, Bouarifi W, Bensikaddour D. Image Restoration Using a Reaction-Diffusion Process. Electronic Journal of Differential Equations. 2014; 2014(197): 1–12.
12. Al-hamzah B, Yebari N. Global existence for reaction-diffusion systems modeling ions electro-migration through biological membranes with mass control and critical growth with respect to the gradient. Topological Methods in Nonlinear Analysis. 2019; 53(1).
13. Al-hamzah B, Yebari N. Gobal Existence in Reaction Diffusion Nonlinear Parabolic Partail Differntial Equation in Image Processing. Global Journal of Advanced Engineering Technologies and Sciences. 2016; 3(5).

14. Dall'Aglio A, Orsine L. Nonlinear parablic equations with natural growth conditions and L^1 data. Nonlinear Anal. T. M. A. 1996; 27(1): 59–73.
15. Morfu S. On some applications of diffusion processes for image processing. Physics Letters A. 2009; 373(29): 24–44.
16. Barbu T, Moroşanu C. Image Restoration using a Nonlinear Second-order Parabolic PDE-based Scheme. Analele ştiinţifice ale Universităţii "Ovidius" Constanţa. Seria Matematică. 2017; 25(1): 33–48.